GEOPHYSICAL RESEARCH LETTERS, VOL. 23, NO. 24, PAGES 3631-3634, DECEMBER 1, 1996

Satellite observations of atmospheric variances: A possible indication of gravity waves

D. L. Wu and J. W. Waters

Jet Propulsion Laboratory, California Institute of Technology, Pasadena

Abstract. The Microwave Limb Sounder (MLS) on the Upper Atmosphere Research Satellite has now produced the first global maps of small-scale variances in the middle atmosphere. Initial analyses are presented here that suggest these variances are due to gravity waves, and the technique used to extract gravity wave information from saturated radiance measurements is described. Observations at 30-80km altitudes show that the variances of horizontal scales less than ~100km are strongly correlated with upper tropospheric convection, surface topography and stratospheric jetstreams. MLS monthly averages during solstice periods suggest that the normalized variance amplitude grows exponentially with height in the stratosphere, and saturates in the mesosphere as expected from wave breaking and dissipation at these altitudes.

Introduction

Internal gravity waves (IGWs), due to buoyancy forces in Earth's atmosphere, play a fundamental role in driving global circulations and determining thermal/constituent structures [Lindzen 1981; Matsuno 1982; Holton 1982; Dunkerton 1984]. Because of small horizontal wavelengths (10-1000km), IGWs can produce significant momentum and energy fluxes through wave breaking, and affect global-scale flows. However, gravity wave forcings are not yet well quantified because adequate global long-term observations are lacking. This uncertainty poses problems for modeling atmospheric general circulations and constituent mixings, particularly in regions, such as the mesosphere and the polar stratosphere, where IGW forcings are relatively strong. Measuring 10-1000km scale atmospheric variations at 20-80km altitudes has been a challenge to modern observational techniques. For ground-based radar techniques [Meek et al. 1985; Vincent and Fritts 1987; Fukao et al. 1994], this altitude region is either too high or low to have sufficient backscattered signals. Most information on IGWs in this region has been provided by rocket soundings [Hirota 1984; Eckermann et al. 1994] and lidar measurements [Wilson et al. 1991] which are limited to a few geographic locations. Satellite remote-sensing has previously provided global measurements of planetary [Rodgers 1976] and large-scale (100's km) waves [Fetzer and Gille 1994], but not of much smaller scale features because of spatial averaging and sparse sampling.

Paper number 96GL02907.
0094-8534/96/96GL-02907$05.00

The study presented here shows that the Upper Atmosphere Research Satellite (UARS) Microwave Limb Sounder (MLS) [Waters 1993; Barath et al. 1993], although not designed for this purpose, can observe small-scale temperature fluctuations at 30-80km altitudes. We obtain the first global maps of variances at small (<100km) horizontal and long (>10km) vertical scales which can be well explained by propagating gravity waves. These results provide new information on gravity wave distribution, generation, propagation and interactions with background atmospheric flows.

Measurement and Analysis

The MLS instrument has been measuring pressure, temperature and constituents since September 1991 by step-scanning the atmospheric limb in ~65 seconds from 90km to the surface, at increments of ~5km in the mesosphere and 1-3km in the stratosphere and troposphere. Figure 1 shows the radiance profiles from a single scan measured by the MLS 63GHz radiometer which resolves the O_2 emission line into 15 spectral channels to retrieve atmospheric tangent pressure and temperature [Fishbein et al. 1996]. All radiances are saturated when the instrument views tangent heights below ~18km, and radiances near line-center (channel 8) saturate at higher altitudes than those near the line-wing (channels 1 and 15) because of stronger line-center absorption. The saturated radiance is a good measure of atmospheric temperature and depends little on the tangent height of the observing path. As the satellite moves along, fluctuations in the saturated radiance profiles reflect atmospheric temperature variations in the horizontal direction.

Instrument spatial resolution and sampling are key to sensing IGW-scale disturbances. Figure 2 gives the temperature weighting functions for 18km tangent height observations, showing eight altitude layers (with thickness of ~10-15km) that contribute to the saturated radiances of different channels. Because the MLS observation direction is perpendicular to the orbit velocity, horizontal averagings are ~100-300km cross-track (perpendicular to suborbit path) due to radiative transfer through the limb path, and ~30km along-track (parallel to suborbit path) due to the antenna field-of-view averaging. These instrumental averagings make MLS most sensitive to long-vertical-wavelength waves having a propagating direction parallel to the suborbit track. For example, in the tropics, MLS is more sensitive to waves propagating in the meridional direction than in the zonal direction. Because of the averagings, amplitudes of the MLS radiance fluctuations are much smaller than the temperature variations measured by high resolution aircraft/rocket sensors,

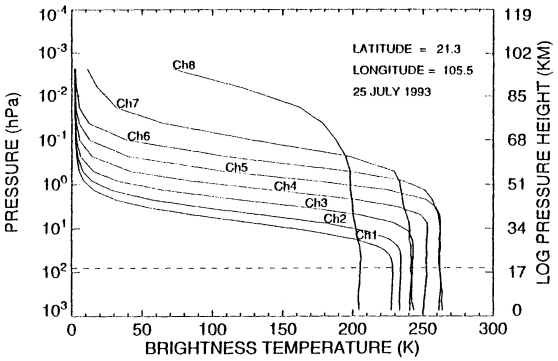

Figure 1. O_2 radiance measurements near 63 GHz as MLS step-scans from the mesosphere to the surface. Fluctuations in the saturated radiances are the effect of atmospheric temperature oscillations and instrument noise.

but are detectable due to low radiometer noise (varying from 0.06K for channels 1 and 15, to 0.5K for channel 8). The integration time for each measurement is ~2 seconds, corresponding to ~14km along-track spatial sampling.

The atmospheric temperature variances can be derived from 6 consecutive measurements of the saturated 63GHz radiance in the bottom of each scan [Figure 1]. The variances calculated for each individual channel correspond to temperature variations at a specified altitude layer as illustrated in Fig.2. These atmospheric fluctuations reveal mainly the disturbances of horizontal scales less than 100km, and we adopt the common interpretation of fluctuations at these scales as a manifestation of upward propagating gravity waves [Hines 1960]. A weak linear variation is first removed from the 6 radiance measurements, which accounts for the tangent pressure dependence and large-scale wave modulations. Subsequently, the total variance of the radiance for a given channel, σ^2, is defined as

$$\sigma^2 = \frac{1}{4}\sum_{i=1}^{6}(y_i - a - bz_i)^2 \qquad (1)$$

where y_i and z_i denote, respectively, measured radiances of the channel and tangent heights. Parameters a and b are determined from the linear least squares fit to the 6 measurements, and 4 is the degree of freedom. The total radiance variance is mainly due to atmospheric temperature fluctuations, instrument noise and non-linear terms of the pressure variation, namely,

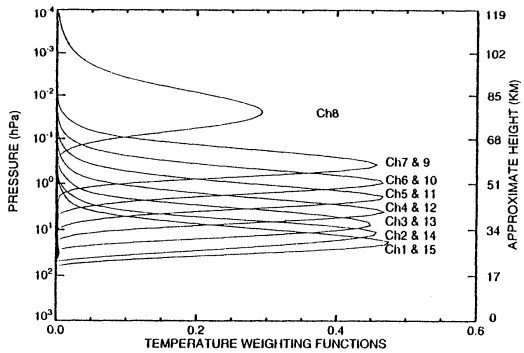

Figure 2. Temperature weighting functions of channels 1-15 for the MLS 63GHz radiometer viewing the limb at 18km (calculated by W. G. Read).

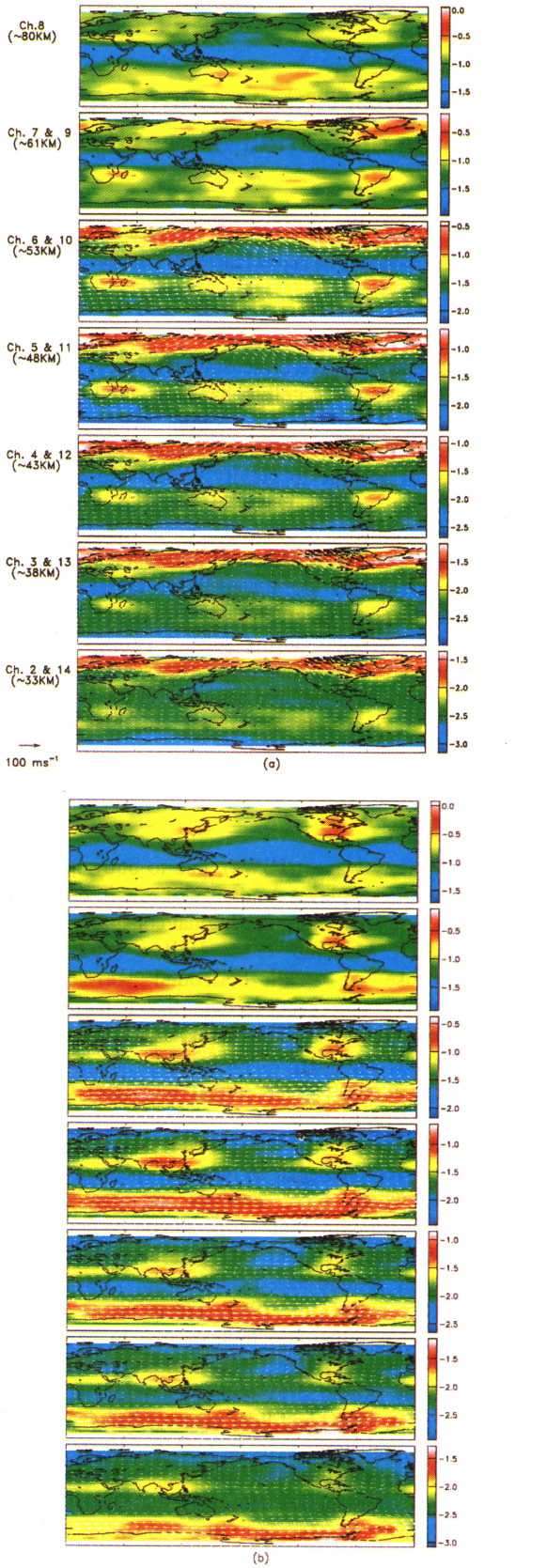

Figure 3. Maps of gravity wave variances observed during (a) January and (b) July. Latitude and longitude bins are respectively 5° and 10° with more than 60 measurements in each grid point. The variances are in a unit of K^2 and colored in a logarithmic scale, i.e., $\log_{10}(\sigma'_{GW})$. Winds (up to ~1 hPa) are derived from the US National Meteorological Center data [Manney et al. 1994] and averaged over the same periods.

$$\sigma^2 = \sigma_{GW}^2 + \sigma_N^2 + \sigma_{NL}^2 \quad (2)$$

where σ_N^2 is the variance due to instrument noise for the given channel that is known from instrument calibrations performed within each limb scan. The non-linear pressure contribution, σ_{NL}^2, is only important for channels 1/15 and 2/14, and can be reasonably estimated from radiance modeling. As a result, the atmospheric fluctuation, σ_{GW}^2, is derived. We repeat the same procedure for all the radiance channels and average the results from the wing channel pairs that correspond to the same altitude layer. Other fluctuation sources, such as the antenna pointing, are either insignificant or very occasional and, therefore, neglected in the analysis here.

Global Maps of Gravity Wave Variance

MLS sampling covers latitudes from 34° in one hemisphere to 80° in the other, and UARS makes 10 yaw maneuvers per year allowing alternating views of high latitudes in the two hemispheres. The variance maps presented here are 40-day averages for two periods near solstices: January (20 December 1992 - 29 January 1993) and July (18 June to 28 July 1993), centered on yaw days. Figure 3 shows the resulting maps at seven altitudes, and striking features in these maps are large amplitudes associated with the stratospheric polar vortex in the winter hemisphere and subtropical land masses in the summer hemisphere. These features evolve with height and change remarkably above the stratopause.

Background winds are expected to play a major role in determining the IGW variance amplitudes observed with MLS. Theoretical studies [Schoeberl and Strobel 1984; Miyahara et al. 1987] show that a strong background wind is a favored condition for IGWs to propagate vertically because then the large intrinsic phase speed (i.e. difference between horizontal wave phase speed and the background wind) prevents the waves from breaking. One may interpret the enhanced variance associated with the stratospheric polar jet as the result of vertically propagating gravity waves. This interpretation is supported by aircraft observations in the lower stratosphere [Hartmann et al. 1989], where a positive correlation was found between small-scale static stability and wind speed. The selective filtering of the jet will shape the wave spectrum differently by allowing upstream propagating IGWs to grow more efficiently with height than others, likely causing the variance enhancement observed in the jetstream. However, horizontal finestructures due to geostrophic adjustment of the jetstream can contribute to the variance observed by MLS, but we cannot quantify this contribution at present. Moreover, the subtropical variances in the summer hemispheres also suggest this filtering effect by background winds, showing larger amplitudes at the latitudes (10°S-30°S in January and 10°N-30°N in July) where winds are stronger. The distribution of these summer IGW variances is consistent with that of the high-wavenumber momentum flux calculated from the GFDL SKYHI high-resolution general circulation model [Miyahara et al. 1987], both enhanced over Madagascar, Australia, South Pacific and Brazil during January.

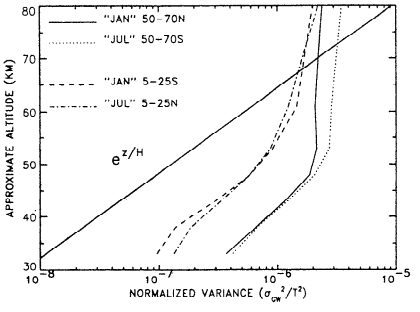

Figure 4. Variance growth at different latitudes during "January" and "July" compared with the exponential growth expected for non-breaking gravity waves. The variances are normalized by the squared mean radiance brightness temperature.

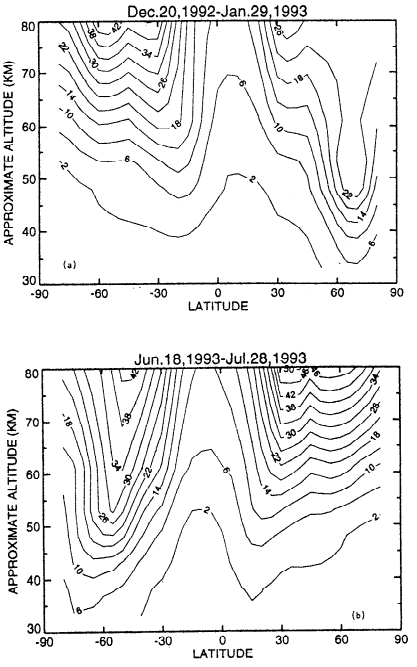

Figure 5. Zonal mean normalized IGW variances for "January" (top) and "July" (bottom). Contours are in units of 10^{-7}.

The spatial distribution of variances shown in Figure 3 also provide certain information on gravity wave sources such as tropospheric convection and surface topography. Tropospheric cumulus convection, frequently occurring in the summer over tropical and subtropical land masses, is most likely responsible for the large stratospheric variances observed near Madagascar, North Australia and Brazil during January, and South Asia, Central America and North Africa during July. However, not all convectively-generated gravity waves can propagate into the stratosphere because of background wind conditions. As discussed above, the prevailing subtropical winds may play an important role to allow only some convective disturbances to reach the stratosphere. Topography related variances can be seen clearly in the results from channels 8 and 7/9, for example, the enhancement over Europe, Asia and America during January and July, and the large variances over Andes during July. The zonal asymmetries of the wintertime jetstreams in the stratosphere are generally believed due to differences in surface topography and tropospheric forcings between the two hemispheres, and IGWs may provide a considerable contribution to such structures.

The height variation of the normalized variance (Figure 4) reveals some important aspects of the propagating nature of the observed perturbations. Despite very different amplitudes in the lower stratosphere, these variances exhibit approximately the same growth rate with height throughout the stratosphere, which is consistent with the theoretical exponential growth for non-breaking IGWs and rocket observations [Hirota and Niki 1985]. This property in variance growth further supports the gravity wave interpretation of the radiance variance observations. Saturation of the normalized variances is observed in the mesosphere, implying generation of wave-induced momentum drag and heat forcing at these altitudes [Fritts 1984]. In Figure 5, zonal means of the normalized variances show that the saturation occurs lower over the stratospheric jetstreams (50°N-70°N in January and 50°S-70°S in July) and subtropical land masses (10°S-30°S in January and 10°N-30°N in July). This suggests that the stratospheric jets would be closed at somewhat lower altitudes in these places, consistent with the structure of climatological mean zonal winds during these periods [Fleming et al. 1990]. Moreover, strong dynamic heating from the IGW saturation in the jetstreams may reverse the temperature lapse rate remarkably and create temperature inversion layers in the mesosphere. Recent maps of temperature inversions in the mesosphere [Leblanc et al. 1995] show a similar distribution to what is observed with the MLS variance maps in the stratosphere.

The new global view of IGWs in the middle atmosphere significantly improves our knowledge of gravity wave generation and propagation, and provides an observational basis for refining IGW parameterization schemes used in atmospheric circulation modeling. Further analyses of MLS radiances are underway and will provide a more complete climatology of global long-term gravity wave activity in the stratosphere and mesosphere.

Acknowledgments. We thank Drs. James Holton and Joan Alexander for helpful conversations on interpretation of the variance observations. We are also indebted to our MLS colleagues, especially G. L. Manney for providing wind data, W. G. Read for calculating weighting functions, and L. Froidevaux, L. S. Elson, R. F. Jarnot, D. A. Flower, E. F. Fishbein and R. R. Lay for helpful discussions. This work was performed at the Jet Propulsion Laboratory, California Institute of Technology, under contract with the National Aeronautics and Space Administration.

References

Barath, F.T., et al., The Upper Atmosphere Research Satellite Microwave Limb Sounder instrument, *J. Geophys. Res.* **98**, 10,751-10,762, 1993.

Dunkerton, T. J., Inertia-gravity waves in the stratosphere, *J. Atmos. Sci.*, **41**, 3396-3404, 1984.

Eckermann, S., I. Hirota, and W. K. Hocking, Gravity wave and equatorial wave morphology of the stratosphere derived from long-term rocket soundings, *Q. J. R. Meterol. Soc.*, **121**, 149-185, 1994.

Fetzer, E.J., and J.C. Gille, Gravity wave variance in LIMS temperatures. Part I: Variability and comparison with background winds. *J. Atmos. Sci.*, **51**, 2461-2483, 1994.

Fishbein, E. F., R.E. Cofield, L. Froidevaux, R.F. Jarnot, T. Lungu, W.G. Read, Z. Shippony, J.W. Waters, I.S. McDermid, Validation of UARS MLS temperature and pressure measurements, *J. Geophys. Res.*, in press, 1996.

Fleming, E. L., S. Chandra, J. J. Barnett, and M. Corney, Zonal mean temperature, pressure, zonal wind and geopotential height as functions of latitudes. *Adv. Space Res.*, **10**, 11-59, 1990.

Fritts, D.C., Gravity wave saturation in the middle atmosphere: A review of theory and observations. *Rev. Geophys.*, **22**, 275-308, 1984.

Fukao, S., M.D. Yamanaka, N. Ao, W.K. Hocking, T. Sato, M. Yamamoto, T. Nakamura, T. Tsuda, and S. Kato, Seasonal variability of vertical eddy diffusivity in the middle atmosphere, 1. three-year observations by the middle and upper atmosphere radar. *J. Geophys. Res.*, **99**, 18,973-18,987, 1994.

Hartmann, D. L., K. R. Chan, B. L. Gary, M. R. Schoeberl, P. A. Newman, R. L. Martin, M. Loewenstein, J. R. Podolske, and S. E. Strahan, Potential vorticity and mixing in the south polar vorex during spring. *J. Geophys. Res.*, **94**, 11,625-11,640, 1989.

Hines, C. O., Internal gravity waves at ionospheric heights. *Can. J. Phys.*, **38**, 1441-1481, 1960.

Hirota, I., Climatology of gravity waves in the middle atmosphere. *J. Atmos. Terr. Phys.*, **46**, 767-773, 1984.

Hirota, I., and T. Niki, A statistical study of inertia-gravity waves in the middle atmosphere. *J. Meteor. Soc. Japan*, **63**, 1055-1066, 1985.

Holton, J.R., The role of gravity wave induced drag and diffusion in the momentum budget of the mesosphere. *J. Atmos. Sci.*, **39**, 791-799, 1982.

Leblanc, T., A. Hauchecorne, M.-L. Chanin, C. D. Rodgers, F. W. Taylor, and N. J. Livesey, Mesospheric temperature inversions as seen by ISAMS in December 1991. *Geophys. Res. Lett.*, **22**, 1485-1488, 1995.

Lindzen, R.S., Turbulence and stress owing to gravity wave and tidal breakdown, *J. Geophys. Res.*, **86**, 9707-9714, 1981.

Manney, G. L., R. W. Zurek, M. E. Gelman, A. J. Miller and R. Nagatani, The anomalous Arctic lower stratospheric polar vortex of 1992-1993. *Geophys. Res. Lett.*, **21**, 2405-2408, 1994.

Matsuno, T., A quasi one-dimensional model of the middle atmosphere circulation interacting with internal gravity waves. *J. Meterol. Soc. Jpn.*, **60**, 215-226, 1982.

Meek, C. E., I. M. Reid, and A. H. Mason, Observations of mesospheric wind velocities 2. Corss sections of power spectral density for 48-8 hours, 8-1 hours, and 1 hour to 10 min over 60-110km for 1981. *Radio Sci.*, **20**, 1383-1402, 1985.

Miyahara, S., Y. Hayashi and J. D. Mahlman, Interactions between gravity waves and planetary-scale flow simulated by the GFDL SKYHI general circulation model. *J. Atmos. Sci.*, **43**, 1844-1861, 1987.

Rodgers, C. D., Evidence for the five-day wave in the upper stratosphere. *J. Atmos. Sci.*, **33**, 710-711, 1976.

Schoeberl, M. R., and D. F. Strobel, Nonzonal gravity wave breaking in the winter mesosphere. *Dynamics of the Middle Atmosphere*, J.R. Holton and T. Matsuno, Eds. (Terra, Tokyo, 1984), pp.45-64.

Vincent, R.A., and D.C. Fritts, A climatology of gravity wave motions in the mesopause region at Adelaide, Australia. *J. Atmos. Sci.*, **44**, 748-760, 1987.

Waters, J. W., Chap.8 in *Atmospheric Remote Sensing Microwave Radiometry*, M.A. Janssen, Ed., Wiley, New York, pp.383-496, 1993.

Wilson, R., M.L. Chanin, and A. Hauchecorne, Gravity waves in the middle atmosphere observed by Rayleigh Lidar: 2. Climatology. *J. Geophys. Res.*, **96**, 5169-5183, 1991.

D. L. Wu and J. W. Waters, Mail Stop 183-701, Jet Propulsion Laboratory, California Institute of Technology, 4800 Oak Grove Drive, Pasadena, CA 91109. (e-mail: dwu@camel.jpl.nasa.gov)

(Received: January 12, 1996; revised July 2, 1996; accepted July 2, 1996.)